Journal of Structural Biology **127,** 240–247 (1999)
Article ID jsbi.1999.4170, available online at http://www.idealibrary.com on IDEAL®

Polymerase Activities and RNA Structures in the Atomic Force Microscope

Helen G. Hansma,[1] Roxana Golan, Wan Hsieh, Sarah L. Daubendiek,* and Eric T. Kool*

*Department of Physics, University of California, Santa Barbara, Santa Barbara, California 93106-9530; and *Department of Chemistry, University of Rochester, Rochester, New York 14627-0216*

Received March 10, 1999, and in revised form August 6, 1999

The structures of the reaction products are the basis for novel polymerase assays using the atomic force microscope (AFM). Polymerases are the enzymes involved in transcription and replication of DNA. Rapid semiquantitative estimates of the activity of DNA polymerases such as Sequenase, *Taq* polymerase, and AMV reverse transcriptase and RNA polymerases (RNAP) such as *Escherichia coli* RNAP were obtained from AFM images of the nucleic acids after polymerase reactions. DNA polymerases were assayed via replication of the single-stranded ϕX-174 virion. RNAP was assayed via transcription, using a rolling circle DNA template that produces long strands of RNA. In some cases, AFM was better than agarose gel electrophoresis for assaying DNA polymerase activity, since aggregation prevented the DNA from entering the agarose gel. Extended molecules of single-stranded RNA synthesized with the rolling circle DNA template showed varied conformations and degrees of stretching. Some structural differences were observed between two RNAs—a ribozyme concatamer and an RNA with 90% purines.

Key Words: **AFM; AMV reverse transcriptase; DNA rolling circle; enzyme assay; replication; ribozyme; Sequenase; scanning force microscope; SFM; scanning probe microscopy; SPM; *Taq* polymerase; transcription.**

INTRODUCTION

For several years now our laboratory and others have been investigating enzymatic activities with the atomic force microscope (AFM). These investigations have ranged from very difficult observations of real-time single-molecule enzymology to simple imaging of reaction mixtures in air.

We have found that simple imaging of reaction mixtures is convenient for semiquantitative assays of polymerases. Structural differences between the reactants and the products give a rapid visual estimate of the extent of the reaction. Activities of DNA polymerases can also be estimated conveniently on agarose gels, but the activity of RNA polymerase (RNAP) can generally be assayed only with the use of radioactive nucleotides. The nonradioactive AFM assay for RNA polymerase activity uses small circular DNAs or "rolling circles." Small circular DNAs have recently been shown to act as templates for RNA polymerases (Daubendiek and Kool, 1997; Daubendiek *et al.,* 1995; Diegelman and Kool, 1998; Kool, 1996).

Rolling circle DNA templates of two different sequences were used to generate RNAs for AFM imaging. One DNA circle is the template for a ribozyme RNA, which has extensive intramolecular base pairing. The other DNA circle is the template for an RNA sequence with 90% purines. This RNA is capable of only limited Watson–Crick base pairing. Structural differences between these two RNAs were observed in the AFM. These structural differences were different from the structures anticipated from their sequences.

With the AFM, one can take a reaction mixture from a test tube, prepare a sample on mica, and image it in the AFM in ca. 15 min. Samples can be imaged at a rate of ca. 3–4/h, with the capture of two to four images per sample. This rate of sample screening was achieved for many of the 68 condensed DNA samples described previously (Hansma *et al.,* 1998b). DNA was seen in 91% of the samples, even though these samples were prepared in saline, which is not generally ideal for AFM of DNA.

This practical use of AFM adds to a growing list of applications for AFM of DNA, including measurements of DNA bending and looping (Cary *et al.,* 1997; Erie *et al.,* 1994; Han *et al.,* 1997; Hansma *et al.,* 1994; Lyubchenko *et al.,* 1997; Rippe *et al.,* 1997), structures of DNA–protein complexes (Wyman *et al.,* 1995, 1997; Yaneva *et al.,* 1997; Pietrasanta, *et al.,* 1999), nucleosome formation (Allen *et al.,* 1993;

[1] To whom correspondence should be addressed. Fax: (805) 893-8315. E-mail: hhansma@physics.ucsb.edu.

1047-8477/99 $30.00

Bustamante *et al.,* 1997b; Fritzsche and Henderson, 1997), DNA mapping (Allison *et al.,* 1997), and DNA condensation for gene therapy (Dunlap *et al.,* 1997; Fang and Hoh, 1998; Hansma *et al.,* 1998b; Wolfert and Seymour, 1996). In addition, AFM of DNA and enzymes in aqueous buffers is beginning to yield information about the sliding of polymerases along DNA molecules (Bustamante *et al.,* 1997a; Kasas *et al.,* 1997; Guthold, *et al.,* 1999).

MATERIALS AND METHODS

Materials

Mica. Discs of mica (Ruby Muscovite mica; New York Mica Co., New York, NY) were glued to steel discs with 2-Ton epoxy resin (Devcon Corp., Wood Dale, IL) and cleaved with tape immediately before use.

Ni-mica. For some samples, as indicated in the figure captions, the K^+ cations naturally present on the mica surface were exchanged with Ni^+ by placing a 5-μl drop of 1 mM $NiCl_2$ on the surface and washing with Milli-Q water after 1 min (Hansma *et al.,* 1995).

DNAs. ϕX174 DNA virion was obtained from New England BioLabs (Beverly, MA). ϕX174 primer with a sequence of 5′ TCATGGAAGCGATAAAACTC 3′ was provided by R. L. Sinsheimer. The DNA circle used for synthesizing purine-rich RNAs had a pyrimidine-rich sequence of $(5'\text{-GATTCCTTTCTTCTTTCCTTC})_2$ (Daubendiek, 1998; Rubin *et al.,* 1995). The other DNA circle (AH83) was 83 nt long and encoded a repeating hammerhead-motif ribozyme (Daubendiek and Kool, 1997).

Enzymes and chemicals. *Taq* DNA polymerase (5 U/μl) was obtained from Promega (Madison, WI). AMV reverse transcrip-

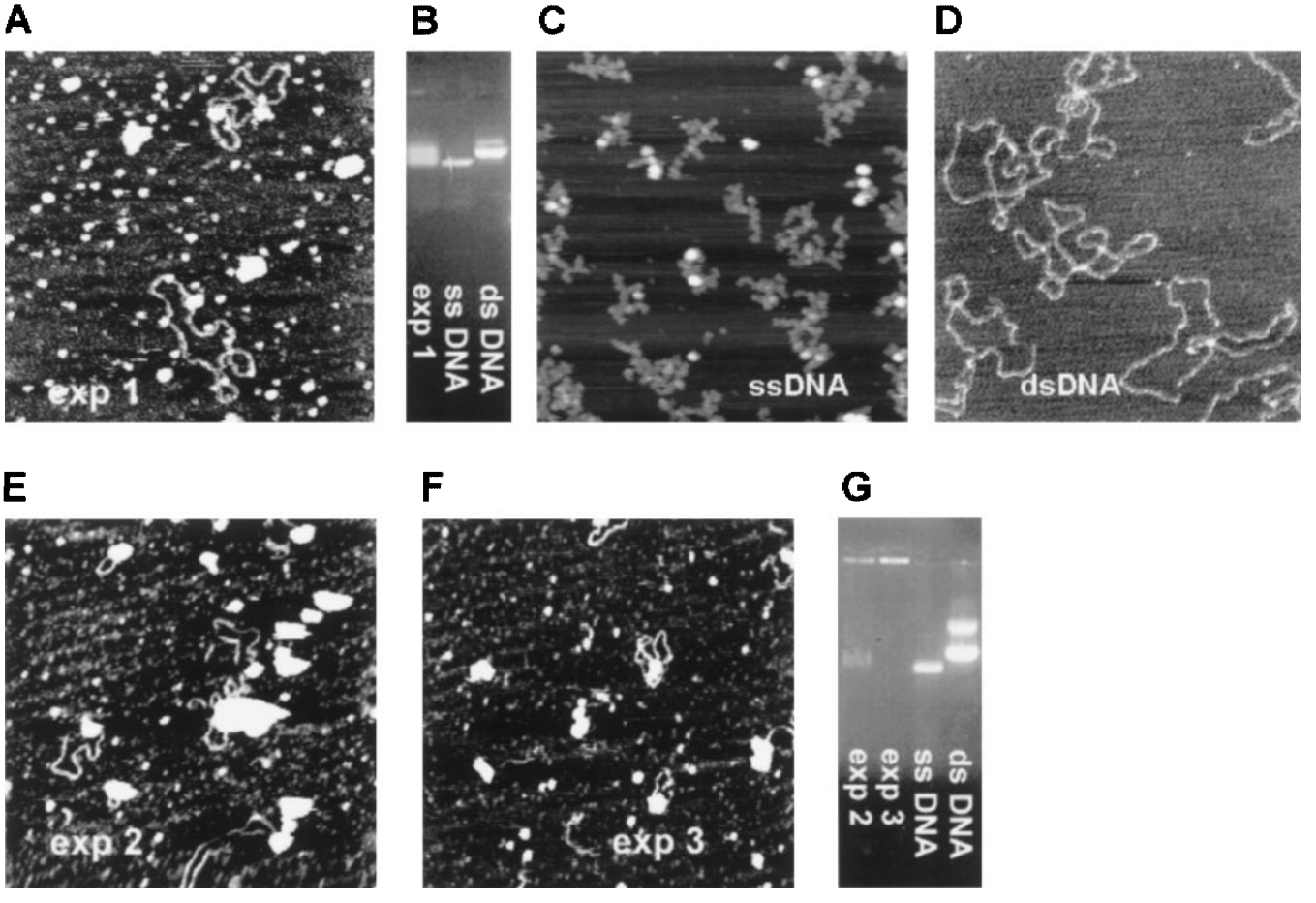

FIG. 1. DNA replication assayed by AFM in aqueous buffers (A, E, F) and by agarose gel electrophoresis (B, G). Single-stranded unreplicated DNA (C, ϕX-174 virion) and replicated DNA (D, ds ϕX-174) are shown in the lanes indicated in the two gels, B and G. Reaction mixtures were incubated for 10 min at 37°C prior to AFM imaging. Aliquots of reaction mixtures were diluted to a final DNA concentration of 1 ng/μl in 10 mM Hepes + 1 mM $NiCl_2$, pH 7. A volume of 35 μl of this diluted reaction mixture was placed on the cantilever in the fluid cell prior to engagement. (A) Replication with AMV reverse transcriptase: The lengths of dsDNA in this AFM image correspond to ca. 50% replication by comparison with the ds ϕX DNA in D. (E, F) Replication with *Taq* polymerase. These AFM images show that a small amount of replication occurred. AFM was on Ni-mica. The corresponding two lanes on the gel (G, lanes 1 and 2) show that most of the DNA has not migrated into the gel, making it impossible to determine the extent of replication by agarose gel electrophoresis. (Exp. 1) The 10-μl reaction mixture contained 1 U AMV reverse transcriptase, 20 nmol dNTPs, and 500 ng primed DNA in 50 mM Tris (pH 8.3), 1 mM DTT, 30 mM KCl, and 8 mM $MgCl_2$. (Exp. 2) The 10-μl reaction mixture contained 1 U *Taq* polymerase, 20 nmol dNTPs, and 500 ng primed DNA in 40 mM Mops (pH 7.4), 10 mM $MgCl_2$, 50 mM NaCl, and 5 mM $MnCl_2$. (Exp. 3) The 10-μl reaction mixture contained 1 U *Taq* polymerase, 20 nmol dNTPs, and 500 ng primed DNA in 50 mM Tris (pH 9.0), 50 mM NaCl, and 10 mM $MgCl_2$. AFM image sizes: 1 μm × 1 μm.

tase (2200 u/ml), dNTPs (100 mM of each nucleotide), and 10× One-Phor-All Buffer (10× OPA, 100 mM Tris–acetate (pH 7.5), 100 mM magnesium acetate, 500 mM potassium acetate) were obtained from Pharmacia Biotech (Piscataway, NJ). Sequenase version 2.0 (13 U/μl) and Sequenase buffer (8 mM Tris–HCl (pH 7.5), 4 mM $MgCl_2$, 10 mM NaCl) were obtained from Amersham (Cleveland, OH). RNasin Ribonuclease inhibitor was obtained from Promega. Histidine-tagged RNAP was provided by M. Kashlev and E. Nudler (Kashlev *et al.,* 1993).

Methods

Preparation of primed DNA. ϕX174 DNA virion (10 pmol) and primer DNA (100 pmol) were diluted in Milli-Q purified water to a final concentration of 300 ng/μl virion DNA. The solution was heated at 65°C for 2 min and cooled to 2°C at a rate of 2°C/min.

Enzymatic reactions. These were carried out under the conditions specified in the figure captions.

AFM imaging. Tapping mode AFM was carried out using a Nanoscope III and MultiMode AFM with a D-scanner (Digital Instruments, Santa Barbara, CA). Leveling of the AFM head was carried out as described previously (Hansma and Laney, 1996).

(i) For AFM in fluid, V-shaped silicon nitride cantilevers, 100 μm long with narrow arms, had tips grown on them by electron beam deposition (Hansma *et al.,* 1992; Keller *et al.,* 1992).

(ii) For AFM in air, 150-μm silicon cantilevers with resonance frequencies of ~300 kHz were used.

Image analysis. Images were processed by flattening to remove the background slope. Molecular and submolecular heights were measured with the Nanoscope Bearing command as follows: A box was drawn to enclose the area of interest. The maximum height in this box was measured. The box was moved to an adjacent area of featureless bare mica, and the maximum height in the box was measured. The height of the feature of interest was calculated by subtracting the background height from the height in the area of interest.

Contour lengths of DNA loops were measured with Dnacalc DNA Processing Application Version 2.5 (Gluschenko Gennadij, Moscow, Russia, gena@nanko.ru; vprokh@ibch.siobc.ras.ru).

Results are expressed as means ± standard deviation (SD).

Gel electrophoresis. DNA samples and aliquots of reaction mixtures were mixed with a solution of 40% (w/v) sucrose in loading buffer with 0.25% bromophenol blue as a tracking dye. The mixture was loaded onto an agarose gel containing ethidium bromide. Electrophoresis was carried out at 70 V.

RESULTS AND DISCUSSION

DNA Polymerases

The activities of DNA polymerases were estimated by imaging stages in the replication of single-stranded DNA (ssDNA) to double-stranded DNA (dsDNA) (Figs. 1 and 2). The ϕX-174 DNA is single-stranded before replication. Replicated DNA was differentiated from unreplicated DNA by the large difference in persistence length. The replicated dsDNA has a relatively large persistence length and a linear appearance (Fig. 1D), while the unreplicated ssDNA has a much shorter persistence length and a highly folded appearance (e.g., Figs. 1C and 2C).

The extent of DNA replication was assayed by AFM in either fluid or air. Aliquots of the polymerase reaction mixture were removed from the test tube after incubation and applied to mica.

The DNA polymerase activities in Figs. 1A, 1E, and 1F were assayed by AFM in fluid. The easiest way to obtain stable images of DNA in aqueous fluids is to add a metal salt such as Ni^{2+} to an aliquot of the reaction mixture and to image the DNA in this buffer (Bezanilla *et al.,* 1994; Hansma and Laney, 1996).

DNA polymerase activity was also detected by applying an aliquot of the reaction mixture onto the mica, rinsing, drying, and imaging in air (Figs. 2B–2E). In these experiments, the polymerase reaction was run in four different buffers that yielded little replication, as seen by both AFM and agarose gel electrophoresis (Fig. 2). The four lanes on the gel in Fig. 2A correspond to the four AFM images in Figs. 2B–2E, left to right. Some replication is seen in the first and third lanes of the gel and in the first and third AFM images in Fig. 2. Little or no replication is seen in the second and fourth gel lanes and AFM images.

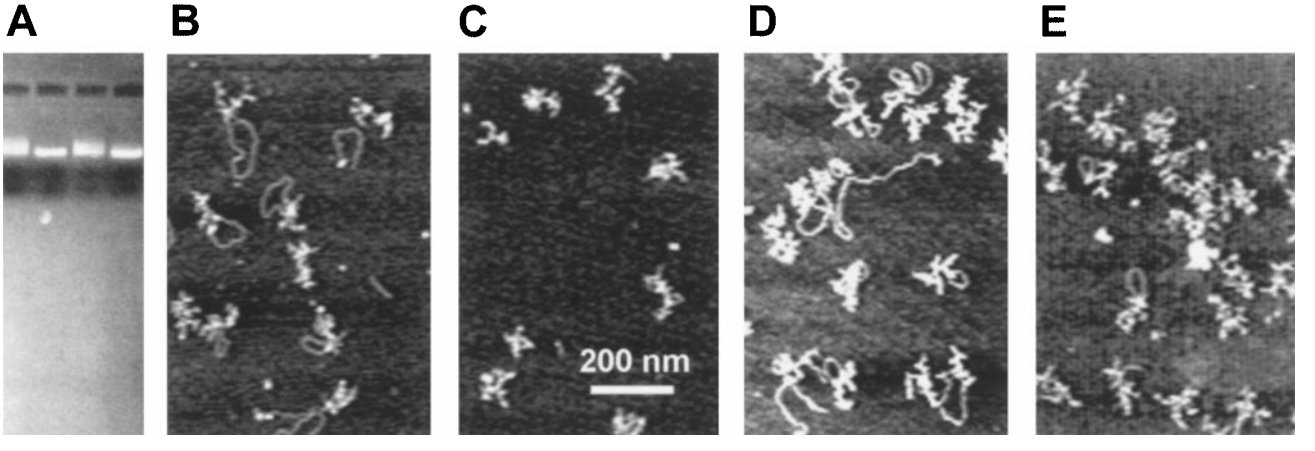

FIG. 2. Comparable levels of replication were seen by agarose gel electrophoresis (A) and by AFM (B–E) in four different buffers where Sequenase activity was minimal. AFM was done in dry helium. Single-stranded ϕX-174 virion DNA was incubated for 13 min at room temperature in a reaction mixture containing Sequenase and one of the following four buffers at pH 7.5 (left to right, gel and AFM images): (A) 40 mM Mops, 10 mM $MgCl_2$, 5 mM $MnCl_2$, 50 mM NaCl; (B) buffer in A without NaCl; (C) buffer in A diluted 1:1 with water; (D) buffer in B, pH 7.9.

AFM in air has an advantage over AFM in buffer for assaying polymerase activities because samples for AFM in air can be stored for imaging at a later time. AFM in air also has a disadvantage over AFM in fluid, however, because the DNA is often removed from the mica surface by rinsing. This variability is probably due to differences in buffers and rinsing forces.

Agarose gel electrophoresis can also be used to estimate the extent of replication and is more readily available in most laboratories. On agarose gels, ssDNA migrates faster than dsDNA, which is larger and less compact (Figs. 1B and 1G). With agarose gel electrophoresis, one estimates the extent of replication of a population of DNA molecules, while with AFM, one observes and measures the extent of replication of individual DNA molecules.

In some cases DNA polymerase activity was detected by AFM (Figs. 1E and 1F) but not by agarose gel electrophoresis (Fig. 1G). An inexpensive *Taq* polymerase was used in this experiment. On the agarose gel, most of the DNA remained at the origin (Fig. 1G), while in the AFM, loops of dsDNA could be seen (Figs. 1E and 1F). The loops of dsDNA seen in the AFM were all attached to large blobs. We hypothesize that these blobs are aggregates of *Taq* polymerase and that the DNA remained at the origin on the agarose gel because the aggregates associated with it were too large to enter the gel.

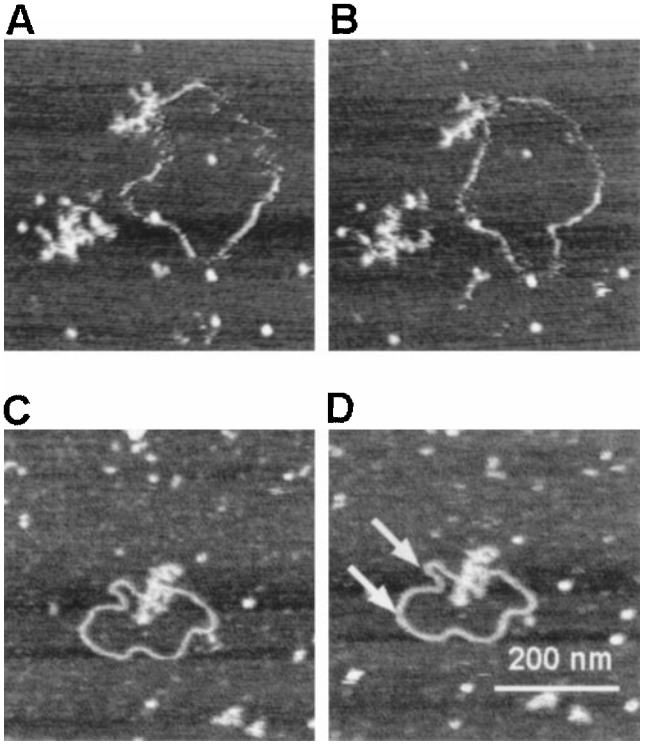

FIG. 3. DNA replicated by Sequenase in the AFM. (A and B) are successive images from one experiment, taken 3.5 min apart; a molecule of ssDNA (ϕX-174 viron) is on the left, and a molecule of partially replicated DNA is on the right. (C and D) are successive images from another experiment, taken 3 min apart, showing a partially replicated DNA molecule bound to the mica such that there were only tiny changes in the DNA conformation with repeated scanning (arrows). Image sizes: 500 nm × 500 nm. Samples were prepared as follows: 600 μM dNTPs and 0.5 ng/μl of primed ϕx-174 virion DNA were preincubated in 100 μl Mn buffer (Sequenase buffer supplemented with 5 mM $MnCl_2$). Mn buffer was injected into the AFM fluid cell with an O-ring onto Ni-mica to adjust the imaging conditions. Once this was done, 0.8 units of Sequenase was added to the reaction mixture, and the reaction mixture was injected into the AFM and imaged (Argaman *et al.,* 1997).

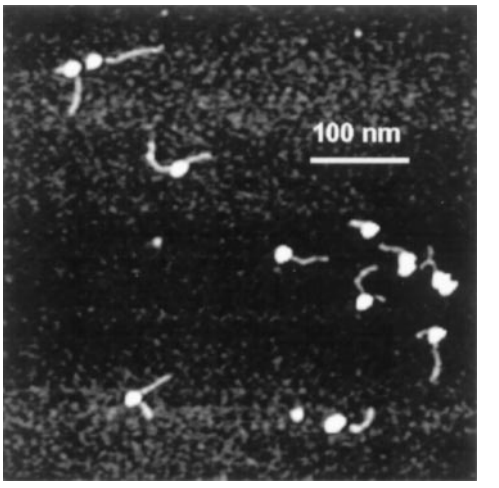

FIG. 4. Stalled elongation complexes of DNA with *Escherichia coli* RNAP. The RNA cannot be seen in these complexes of RNAP with 324-bp DNA (~108 nm long) and 56 nt of RNA. The complexes that stalled with 56 nt of RNA have a DNA arm ratio of ~2:1. Some RNAPs transcribe through this site and remain bound to the end of the DNA. These complexes were prepared with histidine-tagged RNAP bound to a Ni^{2+}-chelating agarose bead that could be washed after successive additions of NTPs to halt the replication at specific points in the nucleotide sequence (Hansma *et al.,* 1998a; Kashlev *et al.,* 1993). AFM was done in dry helium. Image size, 800 nm.

Single-Molecule Enzymology

One goal of these experiments is to improve the imaging of single active molecules of polymerases and other enzymes with the AFM. Single active enzyme molecules are now being observed in several ways, including laser tweezers (Svoboda and Block, 1994; Yin *et al.,* 1995), AFM (Bezanilla *et al.,* 1994; Bustamante *et al.,* 1994; Drake *et al.,* 1989; Kasas *et al.,* 1997), and fluorescence microscopy of single enzyme molecules (Kabata *et al.,* 1993; Moerner, 1997) or their reaction products (Tan and Yeung, 1997).

For AFM, one of the greatest challenges is to find a fluid that supports both the polymerase activity and stable AFM imaging. For Sequenase, a Mn^{2+}-supplemented buffer meets this challenge (Fig. 3) (Argaman *et al.,* 1997). Mn^{2+} partially stabilizes DNA on mica for AFM imaging (Hansma and Laney,

1996) and is sometimes added to Sequenase reaction mixtures used for DNA sequencing. In Fig. 3, unlike in Argaman *et al.* (1997), the replicated DNA remained circular.

DNA motion was sometimes observed. For example, the dsDNA in Figs. 3A and 3B moved a lot and was loosely bound to the mica. In contrast, the dsDNA in Figs. 3C and 3D showed only tiny changes in position (arrows) after continuous scanning for 3 min between Figs. 3C and 3D. This DNA was bound more securely to the mica and gave much clearer images in the AFM.

Loosely bound DNA and tightly bound DNA both showed no measurable replication after adsorbing to mica in the two experiments of Figs. 3A and 3B and Figs. 3C and 3D. Therefore, the replication apparently occurred in the fluid before the Sequenase–DNA complexes adsorbed to the mica. Contact with the mica surface might inactivate Sequenase or prevent the ssDNA from moving through the Sequenase as needed for replication. Sequenase inactivation may be the more serious problem, because ssDNA typically moves on the mica surface for several minutes before binding in a stable conformation as in Fig. 1C. Other polymerases such as *Taq* might be more active on the mica surface.

Such single-molecule enzymology with the AFM continues to be difficult. A radically new approach to this goal is needed. One radical approach is to image active enzymes in organic solvents. Enzymes, when active in organic solvents, are usually much slower than in water (Klibanov, 1997), which would be advantageous for observing enzymatic processes by AFM.

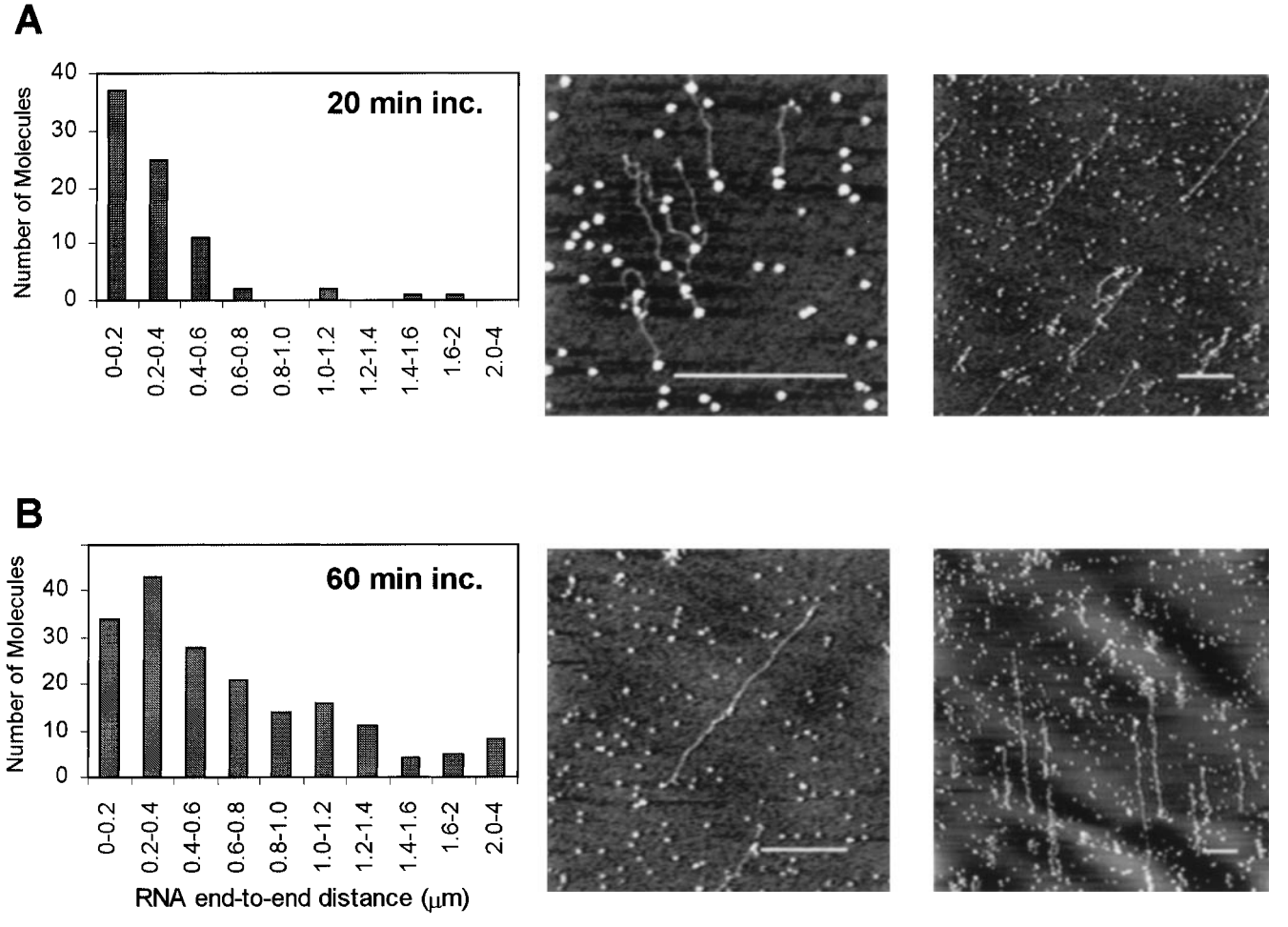

FIG. 5. RNA polymerase activity estimated from AFM images of purine-rich RNA transcribed by *E. coli* RNAP from a rolling circle DNA template. The extent of RNA synthesis is shown in the corresponding histograms. Samples were incubated at 37°C in a test tube for (A) 20 and (B) 60 min before aliquots were applied to mica for AFM in air. Scale bars, 500 nm. Transcription was done as follows: (i) Samples of 10 μl containing 0.2 μM pyrimidine-rich DNA circle and 0.48 μg *E. coli* RNAP in 2× OPA Buffer were incubated for 10 min at 37°C. (ii) An NTP mixture (ATP, CTP, GTP, UTP) at a final concentration of 25 mM for each NTP and RNasin ribonuclease inhibitor was added to the sample, which was again incubated at 37°C. Aliquots for AFM were removed at 20 and 60 min. (iii) 0.3-μl aliquots were pipetted onto freshly cleaved mica. The mica samples were immediately rinsed with H_2O, dried with a stream of compressed air, and further dried in a desiccator over P_2O_5.

RNA Polymerases

The AFM is more useful for assaying RNA polymerases than DNA polymerases because RNA polymerases can be assayed by AFM without the use of radioactivity. Typically, RNA polymerases are assayed by the incorporation of ^{32}P into RNA (Chamberlin, 1982; Lewis and Burgess, 1982), which produces toxic wastes but is more quantitative than AFM.

When the template for RNA polymerase is a linear DNA molecule, the RNA product is not readily measurable by AFM (Hansma *et al.,* 1998a). The elongation complexes in Fig. 4 show RNAP that was stalled on a 324-bp dsDNA after transcribing 56 nucleotides (nt) of RNA (Nudler *et al.,* 1994). The transcribed RNA in Fig. 4 is not visible. The transcribed RNA is also not visible in the time-lapse AFM images of RNAP processing along the DNA template during transcription (Kasas *et al.,* 1997), although of course the objective of that research was to visualize RNAP in action, not to assay the activity of the RNAP.

With a rolling circle DNA template, however, the RNA polymerase transcribes a long strand of RNA that is readily observable by AFM in air (Fig. 5) (Kasas *et al.,* 1997). The extent of RNA synthesis can be estimated by measuring the end-to-end distances of individual RNA strands or by simply observing the AFM images (Fig. 5). The broad distribution of lengths of RNA molecules has been observed also by gel electrophoresis of ^{32}P-labeled RNA synthesized from rolling circle DNA templates (Daubendiek *et al.,* 1995).

RNA Structures

We observed three differences between the structures of purine-rich RNAs and the structures of ribozyme-concatamer RNAs (Figs. 5 and 6).

First, purine-rich RNAs often showed finger-like projections (Figs. 6A and 6D). In contrast, ribozyme RNAs never showed finger-like projections. The finger-like intramolecular substructures in purine-rich RNAs were unexpected because this RNA sequence is capable of forming only 4 Watson–Crick base pairs per 42-nt sequence repeat (Fig. 7). We hypothesize that the fingers are due to a sequence-dependent non-Watson–Crick base pairing in the purine-rich

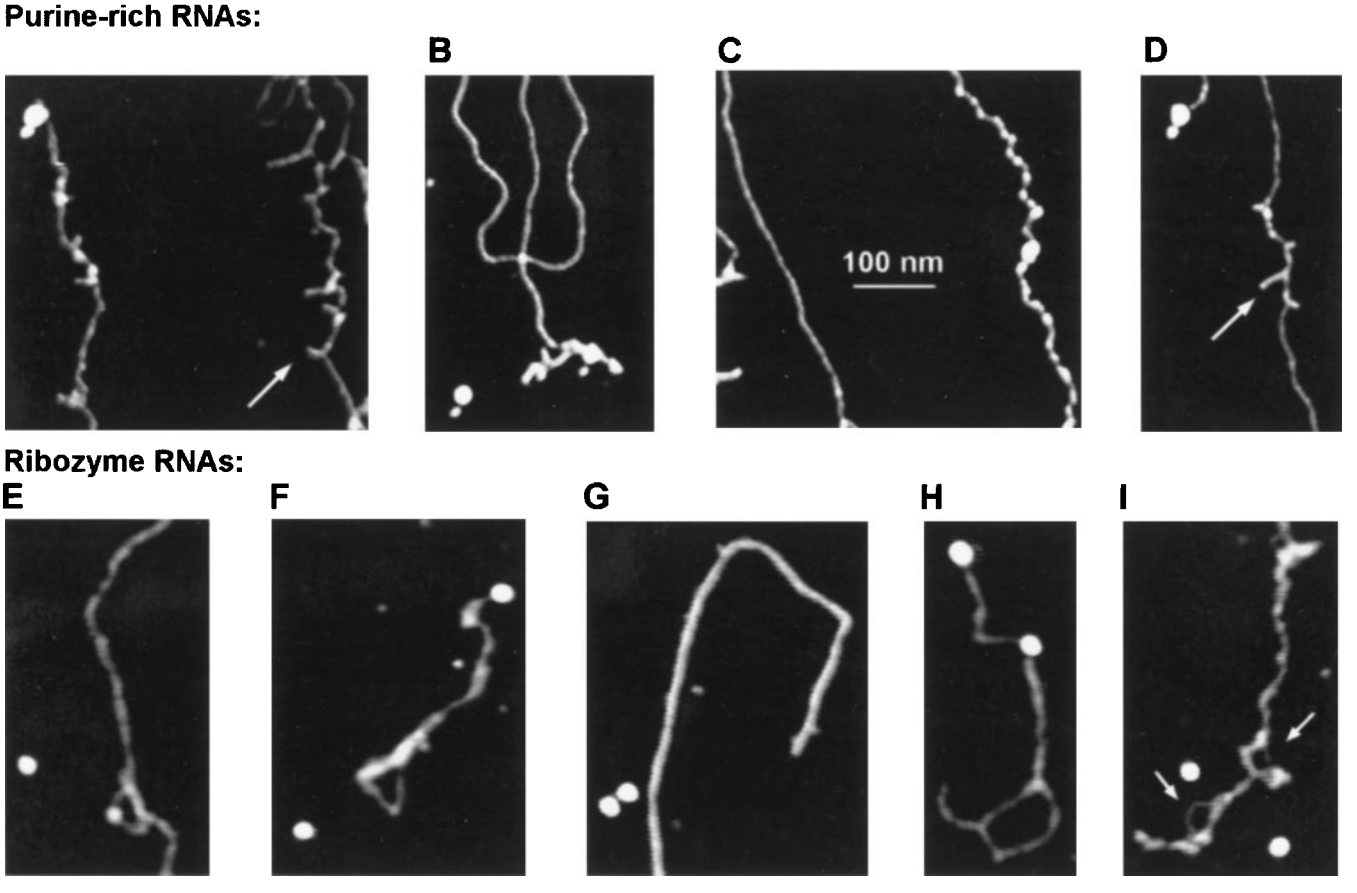

FIG. 6. RNA molecules produced by RNAP with the rolling circle DNA template show a variety of conformations. (A–D) Purine-rich RNA. Arrows in A and D point to selected fingers or hairpins. (E–I) Ribozyme RNA. Arrows in I indicate low, thin regions on RNA. Reaction conditions as in Fig. 5, except that the DNA circle for E–I was the 83-nt ribozyme template. Scale bar, 100 nm.

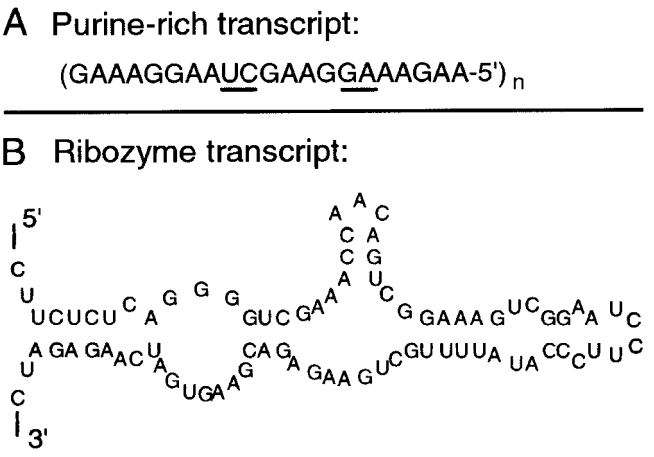

FIG. 7. Sequences of RNA transcripts. (A) Purine-rich RNA shown in Figs. 5 and 6A–6D is a repeating 21-mer. The 4 nt that are underlined form Watson–Crick base pairs as predicted by the software, RNAStructure 3.21 (Mathews *et al.,* 1999). (B) Ribozyme transcript RNA shown in Figs. 6E–6I folds into repeats of this structure (Daubendiek and Kool, 1997).

RNAs. The most frequent finger length was 15–20 nm (30% of fingers), which is approximately the predicted length for 42 nt of RNA. Fingers of this length could form from an anti-parallel arrangement or hairpin between two tandem 42-nt repeats on the purine-rich RNA. Such a hairpin could form anti-parallel heteropurine or homopurine base pairs and 8 Watson–Crick base pairs (Saenger, 1984).

Second, ribozyme RNAs sometimes had short regions that were unusually low (0.3 ± 0.02 nm high), as if short lengths of the RNA were stretched (Fig. 6I, arrows). Regions this low were not seen on purine-rich RNAs. We hypothesize that the purine-rich RNAs have higher stacking energies that inhibit them from being stretched as much as the rizbozyme RNAs, which have only 54% purines (A + G). Purine–purine base stacks are the most stable, followed by mixed purine–pyrimidine stacks, and pyrimidine–pyrimidine stacks are the least stable (Saenger, 1984).

Third, uniformly thick ribozyme RNAs were seen occasionally (1.5 ± 0.1 nm high; Fig. 6G). No uniformly thick purine-rich DNAs were seen, but the finger-like projections and the lumps in purine-rich RNAs were also ~1.5 nm high. The normally extended regions of both RNAs in Fig. 6 were 0.8 ± 0.2 nm high in AFM images. RNAP molecules, for comparison, were 4 ± 0.7 nm high.

Single-stranded molecules of the RNA homopolymer poly(A) resembled the bead-like strand of purine-rich RNA in Fig. 6C, right. The distances between the beads were 15 to 25 nm, center-to-center (Hansma *et al.,* 1996). Single-stranded poly(A) did not exhibit any of the other conformations seen in the ribozyme RNA or the purine-rich RNA, such as extended, tangled, looped, thick, or with projecting fingers of folded RNA.

The ribozyme–template DNA circle was less processive than the pyrimidine-rich DNA circle, judging from the shorter lengths of the RNAs generated with the ribozyme circle. It is possible that the "fingers" seen in purine-rich RNA are seen because the purine-rich RNA is long enough to stretch and twist physically into these finger-like projections, while the ribozyme RNA is too short for such elastic conformational changes to occur during adhesion, rinsing, and drying of the samples on mica.

We thank Scott Hansma for developing NanoConvert, a tiff conversion software for the AFM. We thank Evgeny Nudler, Magdalena Bezanilla, and Mikhail Kashlev for the sample in Fig. 4, Wolfram Saenger for consultation about purine–purine base pairing, and Miriam Argaman for helpful assistance with the rolling circle assays. This work was funded by NSF MCB 9604566 (HH, RG, WH), NSF DMR 9632716 (RG) and Digital Instruments.

REFERENCES

Allen, M. J., Dong, X.-F., O'Neill, T. E., Yau, P., Kowalczykowski, S. C., Gatewood, J., Balhorn, R., and Bradbury, E. M. (1993) Atomic force microscope measurements of nucleosome cores assembled along defined DNA sequences, *Biochemistry* **32,** 8390–8396.

Allison, D. P., Kerper, P. S., Doktycz, M. J., Thundat, T., Modrich, P., Larimer, F. W., Johnson, D. K., Hoyt, P. R., Mucenski, M. L., and Warmack, R. J. (1997) Mapping individual cosmid DNAs by direct AFM imaging, *Genomics* **41,** 379–384.

Argaman, M., Golan, R., Thomson, N. H., and Hansma, H. G. (1997) Phase imaging of moving DNA molecules and DNA molecules replicated in the atomic force microscope, *Nucleic Acids Res.* **25,** 4379–4384.

Bezanilla, M., Drake, B., Nudler, E., Kashlev, M., Hansma, P. K., and Hansma, H. G. (1994) Motion and enzymatic degradation of DNA in the atomic force microscope, *Biophys. J.* **67,** 2454–2459.

Bustamante, C., Erie, D. A., and Keller, D. (1994) Biochemical and structural applications of scanning force microscopy. *Curr. Opin. Struct. Biol.* **4,** 750–760.

Bustamante, C., Rivetti, C., and Keller, D. J. (1997a) Scanning force microscopy under aqueous solutions, *Curr. Opin. Struct. Biol.* **7,** 709–716.

Bustamante, C., Zuccheri, G., Leuba, S. H., Yang, G., and Samori, B. (1997b) Visualization and analysis of chromatin by scanning force microscopy, *Methods* **12,** 73–83.

Cary, R. B., Peterson, S. R., Wang, J., Bear, D. G., Bradbury, E. M., and Chen, D. J. (1997) DNA looping by Ku and the DNA-dependent protein kinase, *Proc. Natl. Acad. Sci. USA* **94,** 4267–4272.

Chamberlin, M. J. (1982) Bacterial DNA-dependent RNA polymerases, *in* The Enzymes, Vol. XV, pp. 61–86, Academic Press, San Diego.

Daubendiek, S. L. (1998) Ph.D. Thesis. University of Rochester, Rochester, NY.

Daubendiek, S. L., and Kool, E. T. (1997) Generation of catalytic RNAs by rolling transcription of synthetic DNA nanocircles, *Nat. Biotechnol.* **15,** 273–277.

Daubendiek, S. L., Ryan, K., and Kool, E. T. (1995) Rolling-circle RNA synthesis—circular oligonucleotides as efficient substrates for T7 RNA polymerase, *J. Am. Chem. Soc.* **117,** 7818–7819.

Diegelman, A. M., and Kool, E. T. (1998) Generation of circular

RNAs and catalytic RNAs by transcription of circular DNA oligonucleotides encoding hairpin ribozymes, *Nucleic Acids Res.* **26,** 3235–3241.

Drake, B., Prater, C. B., Weisenhorn, A. L., Gould, S. A., Albrecht, T. R., Quate, C. F., Cannell, D. S., Hansma, H. G., and Hansma, P. K. (1989) Imaging crystals, polymers, and processes in water with the atomic force microscope, *Science* **243,** 1586–1589.

Dunlap, D. D., Maggi, A., Soria, M. R., and Monaco, L. (1997) Nanoscopic structure of DNA condensed for gene delivery, *Nucleic Acids Res.* **25,** 3095–3101.

Erie, D. A., Yang, G., Schultz, H. C., and Bustamante, C. (1994) DNA bending by Cro protein in specific and nonspecific complexes: Implications for protein site recognition and specificity, *Science* **266,** 1562–1566.

Fang, Y., and Hoh, J. H. (1998) Surface-directed DNA condensation in the absence of soluble multivalent cations, *Nucleic Acids Res.* **26,** 588–593.

Fritzsche, W., and Henderson, E. (1997) Chicken erythrocyte nucleosomes have a defined orientation along the linker DNA—A scanning force microscopy study, *Scanning* **19,** 42–47.

Guthold, M., Zhu, X., Rivetti, C., Yang, G., Thompson, N. H., Kasas, S., Hansma, H. G., Smith, B., Hansma, P. K., and Bustamante, C. (1999) Real-time Imaging of One-dimensional, Diffusion and Transcription by Escherichia coli RNA Polymerase, *Biophys. J.* **77,** in press.

Han, W., Dlakic, M., Zhu, Y. J., Lindsay, S. M., and Harrington, R. E. (1997) Strained DNA is kinked by low concentrations of Zn^{2+}, *Proc. Natl. Acad. Sci. USA* **94,** 10565–10570.

Hansma, H. G., Bezanilla, M., Laney, D. L., Sinsheimer, R. L., and Hansma, P. K. (1995) Applications for atomic force microscopy of DNA, *Biophys. J.* **68,** 1672–1677.

Hansma, H. G., Bezanilla, M., Nudler, E., Hansma, P. K., Hoh, J., Kashlev, M., Firouz, N., and Smith, B. (1998a) Left-handed orientation of histidine-tagged RNA polymerase complexes imaged by atomic force microscopy, *Probe Microsc.* **1,** 117–125.

Hansma, H. G., Browne, K. A., Bezanilla, M., and Bruice, T. C. (1994) Bending and straightening of DNA induced by the same ligand: Characterization with the atomic force microscope, *Biochemistry* **33,** 8436–8441.

Hansma, H. G., Golan, R., Hsieh, W., Lollo, C. P., Mullen-Ley, P., and Kwoh, D. (1998b) DNA condensation for gene therapy as monitored by atomic force microscopy, *Nucleic Acids Res.* **26,** 2481–2487.

Hansma, H. G., and Laney, D. E. (1996) DNA binding to mica correlates with cationic radius: Assay by atomic force microscopy, *Biophys. J.* **70,** 1933–1939.

Hansma, H. G., Revenko, I., Kim, K., and Laney, D. E. (1996) Atomic force microscopy of long and short double-stranded, single-stranded and triple-stranded nucleic acids, *Nucleic Acids Res.* **24,** 713–720.

Hansma, H. G., Vesenka, J., Siegerist, C., Kelderman, G., Morrett, H., Sinsheimer, R. L., Bustamante, C., Elings, V., and Hansma, P. K. (1992) Reproducible imaging and dissection of plasmid DNA under liquid with the atomic force microscope, *Science* **256,** 1180–1184.

Kabata, H., Kurosawa, O., Arai, I., Washizu, M., Margarson, S. A., Glass, R. E., and Shimamoto, N. (1993) Visualization of single molecules of RNA polymerase sliding along DNA, *Science* **262,** 1561–1563.

Kasas, S., Thomson, N. H., Smith, B. L., Hansma, H. G., Zhu, X., Guthold, M., Bustamante, C., Kool, E. T., Kashlev, M., and Hansma, P. K. (1997) *E. coli* RNA polymerase activity observed using atomic force microscopy, *Biochemistry* **36,** 461–468.

Kashlev, M., Martin, E., Polyakov, A., Severinov, K., Nikiforov, V., and Goldfarb, A. (1993) Histidine-tagged RNA polymerase: Dissection of the transcription cycle using immobilized enzyme, *Gene* **130,** 9–14.

Keller, D., Deputy, D., Alduino, A., and Luo, K. (1992) Sharp, vertical-walled tips for SFM imaging of steep or soft samples, *Ultramicroscopy* **42–44** (Pt. B), 1481–1489.

Klibanov, A. M. (1997) Why are enzymes less active in organic solvents than in water? *Trends Biotechnol.* **15,** 97–101.

Kool, E. T. (1996) Circular oligonucleotides: New concepts in oligonucleotide design, *Ann. Rev. Biophys. Biomol. Struct.* **25,** 1–28.

Lewis, M. K., and Burgess, R. R. (1982) Eukaryotic RNA polymerases. *In* The Enzymes, Vol. XV, pp. 111–153, Academic Press, San Diego.

Lyubchenko, Y. L., Shlyakhtenko, L. S., Aki, T., and Adhya, S. (1997) Atomic force microscopic demonstration of DNA looping by GalR and HU, *Nucleic Acids Res.* **25,** 873–876.

Mathews, D. H., Sabina, J., Zuker, M., and Turner, D. H. (1999) Expanded sequence dependence of thermodynamic parameters improves prediction of RNA secondary structure, *J. Mol. Biol.* **288,** 911–940.

Moerner, W. E. (1997) Polymer luminescence—Those blinking single molecules, *Science* **277,** 1059–1060.

Nudler, E., Goldfarb, A., and Kashlev, M. (1994) Discontinuous mechanism of transcription elongation, *Science* **265,** 793–796.

Pietrasanta, L. I., Thrower, D., Hsieh, W., Rao, S., Stemmann, O., Lechner, J., Carbon, J., and Hansma, H. G. (1999) Probing the *Sacchromyces cervisiae* CBF3-*CEN* DNA kinetochore complex using atomic force microscopy, *Proc. Natl. Acad. Sci. USA* **96,** 3757–3762.

Rippe, K., Guthold, M., von Hippel, P. H., and Bustamante, C. (1997) Transcriptional activation via DNA-looping: Visualization of intermediates in the activation pathway of *E. coli* RNA polymerase x sigma 54 holoenzyme by scanning force microscopy, *J. Mol. Biol.* **270,** 125–138.

Rubin, E., Rumney, S. T., Wang, S., and Kool, E. T. (1995) Convergent DNA synthesis: A non-enzymatic dimerization approach to circular oligodeoxynucleotides, *Nucleic Acids Res.* **23,** 3547–3553.

Saenger, W. (1984) Principles of Nucleic Acid Structure, Springer-Verlag, New York.

Svoboda, K., and Block, S. M. (1994) Biological applications of optical forces, *Annu. Rev. Biophys. Biomol. Struct.* **23,** 247–285.

Tan, W. H., and Yeung, E. S. (1997) Monitoring the reactions of single enzyme molecules and single metal ions, *Anal. Chem.* **69,** 4242–4248.

Wolfert, M. A., and Seymour, L. W. (1996) Atomic force microscopic analysis of the influence of the molecular weight of poly(L)lysine on the size of polyelectrolyte complexes formed with DNA, *Gene Ther.* **3,** 269–273.

Wyman, C., Grotkopp, E., Bustamante, C., and Nelson, H. C. M. (1995) Determination of heat-shock transcription factor 2 stoichiometry at looped DNA complexes using scanning force microscopy, *EMBO J.* **14,** 117–123.

Wyman, C., Rombel, I., North, A. K., Bustamante, C., and Kustu, S. (1997) Unusual oligomerization required for activity of NtrC, a bacterial enhancer-binding protein, *Science* **275,** 1658–1661. [See comments].

Yaneva, M., Kowalewski, T., and Lieber, M. R. (1997) Interaction of DNA-dependent protein kinase with DNA and with Ku: Biochemical and atomic-force microscopy studies, *EMBO J.* **16,** 5098–5112.

Yin, H., Wang, M. D., Svoboda, K., Landick, R., Block, S. M., and Gelles, J. (1995) Transcription against an applied force, *Science* **270,** 1653–1656.